PNAS

The role of fire spotting in fire-weather prediction

Maria Frediani[1], Timothy W. Juliano[1], Jason C. Knievel[1], Sarah A. Tessendorf[1], Branko Kosovic[1].

[1]Research Applications Laboratory, National Center for Atmospheric Research, Boulder, CO, 80307-3000.

* Maria Frediani
Research Applications Laboratory
National Center for Atmospheric Research
P.O. Box 3000
Boulder, CO 80307-3000

Email: frediani@ucar.edu

Author Contributions: M. Frediani designed and performed the research, analyzed data, and wrote the paper. T. W. Juliano, J. C. Knievel, S. A. Tessendorf, and B. Kosovic wrote the paper.

Competing Interest Statement: NA.

Classification: Physical Sciences / Earth, Atmospheric, and Planetary Sciences.

Keywords: wildfire, weather, firebrand spotting, ember, fire behavior modeling.

This file includes:
Main Text
Figures 1 to 2

Abstract

This study uses a newly-developed firebrand spotting parameterization in simulations of the Marshall Fire (2021) to demonstrate that without fire spotting, wind-driven fire simulations cannot reproduce the behavior of some fires. The Marshall Fire, the most destructive in Colorado's history, took mere hours to cause nearly half a billion dollars in damage and destroy over 1000 homes. In wind-driven events that occur in the wildland-urban interface, the model's ability to spot is critical for modeling fire spread over water streams and urban features such as highways. Without ignition of fire spots, the simulated Marshall Fire cannot advance. In cases when spotting significantly contributes to fire spread, the process' nonlinear nature is a source of uncertainty to modeling fire behavior that can broaden the model's ensemble spread and possibly produce a more realistic probability of outcomes. The results in this study corroborate the importance of representing fire spotting in atmosphere-fire behavior coupled models, such as WRF-Fire.

Main Text

Introduction

Firebrands are burning pieces of vegetation or organic materials (embers) generated at a fire source and carried with the wind and convection. Fire spotting occurs when firebrands are lofted into the air, land on unburned areas, and ignite new fires. Fires driven by high wind speed combined with low relative humidity and flammable vegetation often result in high fire intensities, rapid growth rates, and showers of embers starting new fires. Intense spotting increases danger to fire crews, affects fire behavior predictability, and challenges suppression efforts and containment methods by fire crews.

Spot fires are considered short-range within a few hundred meters from the source fire, or long-range, with reports of spotting distances as high as 35 km in Australia (1). Short-range spotting accelerates the fire rate of spread by expanding the fire perimeters slightly beyond the fire front (1), whereas long distance spotting can ignite new fires several kilometers downwind, possibly in areas beyond containment boundaries.

Embers play a significant role in spreading wildfires and are of critical importance in the wildland-urban interface. When a fire reaches urban zones, it spreads through two primary mechanisms: (a) adjacent structure ignition, i.e., as structures are consumed, radiant and convective heat may ignite adjacent houses; and (b) ember accumulation, when embers transported by the wind land on flammable structures, leaf-filled gutters, vents, dry lawns, and mulch beds, igniting spot fires near and far ahead. In an urban setting, embers are the leading cause of home ignitions (2).

The Firebrand Spotting parameterization (3) was developed for WRF-ARW model version starting at 4.4. The parameterization uses a Lagrangian particle transport framework to simulate firebrand advection, originating in active fire points determined by WRF-Fire's fire behavior model. The parameterization identifies locations at risk of fire spotting by modeling transport and physical processes of individual firebrands.

In this article, we use numerical simulations to discuss opportunities for an integrated firebrand transport component within a fire-weather coupled community model to advance wildfire research and predictability. This numerical experiment was primarily designed to assess WRF-Fire's ability to simulate the behavior of a fire that was not suppressed. The Marshall Fire started as a grass fire in the outskirts of Boulder, Colorado on 2021/12/30 approx. at 18Z (11 AM MST) and reached the residential area in about 1 hour. The fast spread was driven by extremely high winds from a downslope windstorm, which was described by (4) as "a perfect storm of fast winds and drought conditions as the combination of historically warm temperatures and low precipitation along the Front Range of the Rocky Mountains left the grasses in a state of extreme dryness". To this date, the Marshall Fire is the most destructive in Colorado's State history, with 1084 homes destroyed and 149 damaged (5).

Results

The model experiments for the Marshall fire illustrate the impact of firebrand spotting in the fire behavior simulation along with the caveats of an inaccurate fuel layer.

A comparison between a control simulation (CTRL) and an experiment with four spotting locations (4-spots) is shown in Figure 1, panels A-D. In the CTRL experiment, the fire front is contained by Marshall Rd and Hwy 36 because in the fire fuel layer, these are represented by a no-fuel category.

It is known that fuel layers such as the Anderson 13-fuels (current default in WRF-Fire) and Scott and Burgan 40-fuels, are inaccurate, incomplete, and static over long periods of time (6). The fuels in these layers are simplified representations of various vegetation types, used to parameterize Rothermel's (1972) surface spread equation, and allowing for rapid application in the field, such as during suppression efforts (7). In the region encompassed by our computational domain (Figure 1, panel E), the Anderson 13-fuels classifies urban fuels in a "no-fuels" category (i.e., with fuel load equal to 0 kg/m^2), with the area containing the suburbs burned down by the Marshall Fire represented by short grass, hardwood litter, timber, and closed timber litter (i.e., fuel loads of 0.166, 0.78, 0.896, and 1.12 kg/m^2, respectively). Even though urban structures are misrepresented by the fuel layer, it realistically represents Marshall Rd and Hwy 36. Roads and highways serve as fire containment barriers, with ember transport being the physical process that allows the fire front to advance across the containment. These experiments show that the lack of an integrated spot-fire ignition capability is a critical model limitation.

Even though the 4-spots experiment allowed the model to simulate fire spread across containment barriers, in a case such as the Marshall Fire, four spot fires are a substantial underestimation. Currently, the model limits the number of ignitions to five (in this experiment, one primary ignition, and four spot fires), requiring a CTRL simulation followed by manual configuration of spotting location and ignition time. This is a time-consuming process that is not scalable for producing ensembles, creating datasets for model verification and statistical training sets.

This current model limitation is also detrimental to uncertainty estimation of fire spread, which directly impacts probabilistic skill and our ability to characterize model accuracy. Figure 2 shows three experiments illustrating model sensitivities to rate of spread at initialization (iROS 0.5) and fuel moisture content (fmc 1%, fmc 5%) compared to CTRL (iROS=0.05 and fmc=8%). The snapshots on the left show the fire front arrival time (AT) at Hwy 36. In a dry-fuel experiment (fmc 1%), the AT occurs as early as 19Z, indicating at least three hours of uncertainty due to solely fuel moisture content. The snapshots on the right show the effect of various model parameters at 22Z, corresponding to CTRL's AT. The fire spread and firebrands' response to different model parameters indicate that automated spotting ignitions would be highly nonlinear in both space and time, potentially leading to a broadening of the ensemble spread in probabilistic forecasts. When uncertainty sources are not represented in the model, forecast ensembles generate narrow spreads, reducing the ensemble skill, i.e., its ability to represent the possible outcomes given the input's uncertainty. The Rothermel parameterization and its fuel specification requirements are primary sources of structural and data uncertainty in modeling fire behavior, yet these simulation experiments indicate that firebrand spotting is also an uncertainty source to be considered for improving model accuracy and probabilistic skill.

Discussion

This study uses the Firebrand Spotting parameterization in the WRF model to highlight the impact of firebrand spotting in the fire behavior simulation of the Marshall fire (Colorado, 2021). The parameterization identifies locations at risk of fire spotting but ignition of fire spots is not currently integrated.

Our results show that the model's ability to spot can be critical for modeling fire spread over barriers present in urban and wildland areas, such as highways and water streams. These numerical experiments suggest that underprediction of simulated fire spreads, an issue often attributed to the fire behavior parameterization and fuel data inputs, can be also caused by the presence of containment barriers, which the model is currently unable to breach. Without a spotting capability, numerical models are limited in their role to provide tactical information to operational firefighters, guide land managers, and assist researchers to better understand the various processes and the result of their interactions. In turn, this affects our collective efforts to advance wildfire science, in that the representation of mechanisms of fire spread is incomplete, impacting all stakeholders that directly or indirectly rely on information produced by numerical models.

These numerical experiments also indicate that fire spread and firebrands are spatially and temporally sensitive to parameters and model structure. The interaction between these nonlinear processes can impact the model's ability to represent ensemble spread and probability of outcomes, in that fire spotting can be a significant source of uncertainty to fire behavior that is currently not represented in the model.

Even though WRF-Fire is currently bound by large uncertainties in the fuels and Rothermel parameterization, ensemble simulations and sensitivity tests are essential exercises that enable these structural uncertainties to be partially addressed, improve model predictability, identify and quantify sources, and advance applications, especially those which depend on the interactions between weather and fire.

Materials and Methods

The numerical simulations (8) were produced using WRF-ARW (9) v4.3.3, configured with two nested domains, with 1000 and 111m of horizontal grid spacing, and boundary conditions from the High-Resolution Rapid Refresh (HRRR) model (10). WRF-Fire (11), part of the WRF-ARW modeling system, was used for the fire behavior component. The fuel layer used by WRF-Fire (Anderson 13-fuels) originates from the LANDFIRE database (12). Additional information about the model configuration is provided in the Supporting Information.

Acknowledgments

This material is based upon work supported by the National Center for Atmospheric Research, which is a major facility sponsored by the National Science Foundation under Cooperative Agreement No. 1852977. Partial funding was provided by the U.S. Army Test and Evaluation Command through an Interagency Agreement with the National Science Foundation, which sponsors NCAR.

References

1. M. A. Storey, *et al.*, Experiments on the influence of spot fire and topography interaction on fire rate of spread. *PLoS One* **16**, e0245132 (2021).
2. W. E. Mell, S. L. Manzello, A. Maranghides, D. Butry, R. G. Rehm, The wildland–urban interface fire problem – current approaches and research needs. *Int. J. Wildland Fire* **19**, 238–251 (2010).
3. Jonathan D. Beezley, Janice L. Coen, and Jan Mandel, "User's Guide for the Advanced Research WRF (ARW) Modeling System Version 4.4, Appendix A: WRF-Fire" (UCAR/NCAR, 2022). Available at https://www2.mmm.ucar.edu/wrf/users/docs/user_guide_v4/v4.4/users_guide_chap-fire.html.
4. R. G. Fovell, M. J. Brewer, R. J. Garmong, The December 2021 Marshall Fire: Predictability and Gust Forecasts from Operational Models. *Atmosphere* **13**, 765 (2022).
5. B. Gabbert, Marshall fire updated damage assessment: 1,084 residences destroyed. *Wildfire Today* (2022). Available at https://wildfiretoday.com/2022/01/07/marshall-fire-updated-damage-assessment-1084-residences-destroyed/.

6. A. L. DeCastro, T. W. Juliano, B. Kosović, H. Ebrahimian, J. K. Balch, A Computationally Efficient Method for Updating Fuel Inputs for Wildfire Behavior Models Using Sentinel Imagery and Random Forest Classification. *Remote Sensing* **14**, 1447 (2022).

7. S. “jake” Price, M. J. Germino, Simulation of a historic megafire in sagebrush steppe using FARSITE: inaccuracies resulting from LANDFIRE inputs rectified using readily available vegetation maps derived from satellite imagery (2022) https:/doi.org/10.21203/rs.3.rs-1047854/v1.

8. Computational and Information Systems Laboratory, Cheyenne: SGI ICE XA Cluster (2017) https:/doi.org/10.5065/D6RX99HX.

9. W. C. Skamarock, *et al.*, “A description of the advanced research WRF model version 4” (UCAR/NCAR, 2019) https:/doi.org/10.5065/1DFH-6P97.

10. B. K. Blaylock, J. D. Horel, S. T. Liston, Cloud archiving and data mining of High-Resolution Rapid Refresh forecast model output. *Comput. Geosci.* **109**, 43–50 (2017).

11. J. L. Coen, *et al.*, WRF-Fire: Coupled Weather–Wildland Fire Modeling with the Weather Research and Forecasting Model. *J. Appl. Meteorol. Climatol.* **52**, 16–38 (2013).

12. LANDFIRE, 13 Anderson Fire Behavior Fuel Models (LF 1.4.0) U.S. Department of Interior, Geological Survey, and U.S. Department of Agriculture. Dataset URL https://landfire.gov/fbfm13.php.

Figures

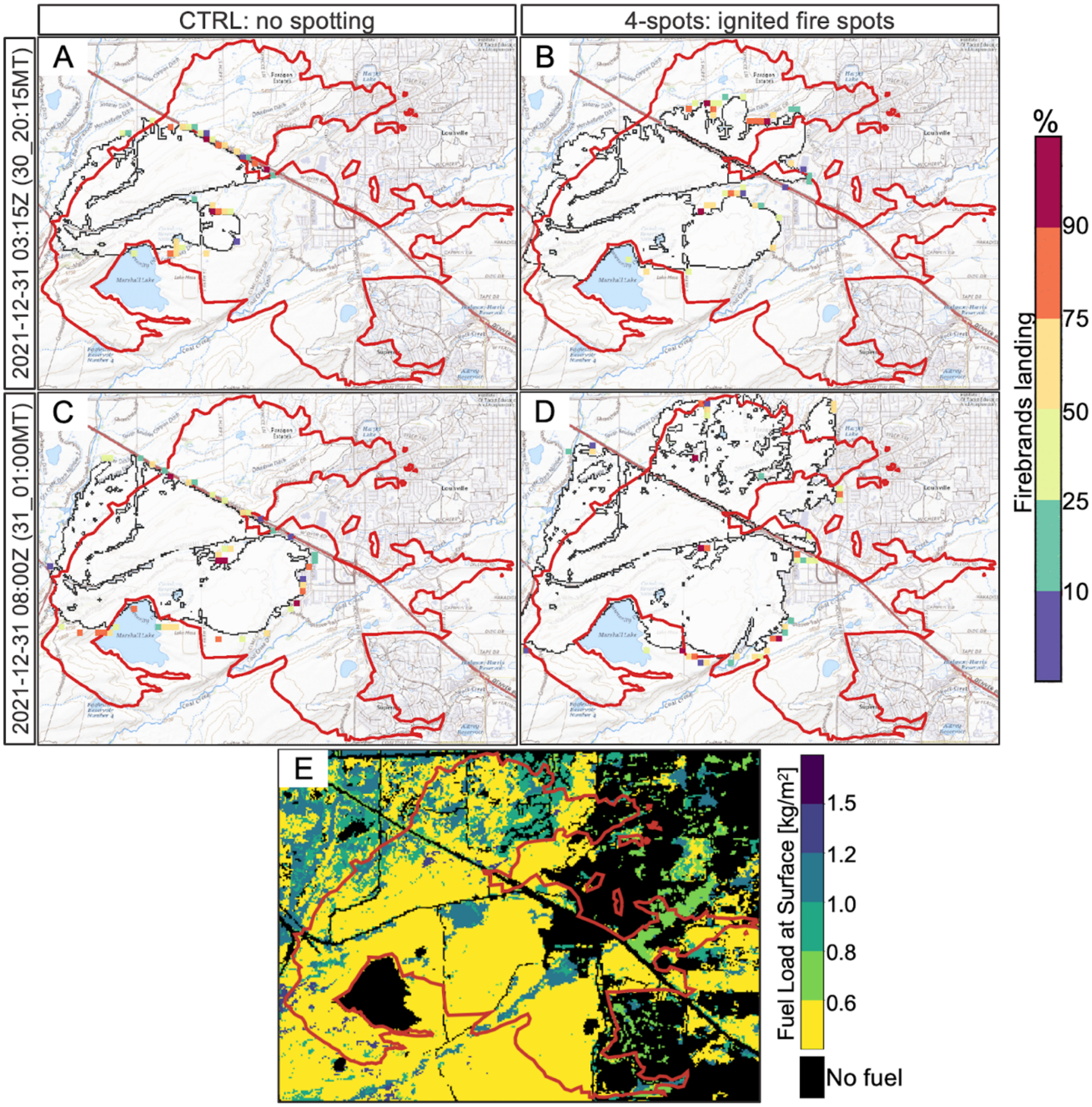

Figure 1. CTRL (A, C) and 4-spots experiment (B, D) at different times into the simulation, and associated fuel load at surface (E). The snapshots in panels A-D show the simulated fire area (black line) and the percentage of firebrands landing ahead of the fire front (colored scale). The 4-spots experiment includes fire spots ignited based on the location and time of firebrand landing density in CTRL. The red line (A-E) indicates the observed fire perimeter after containment (evening of 2021-12-31).

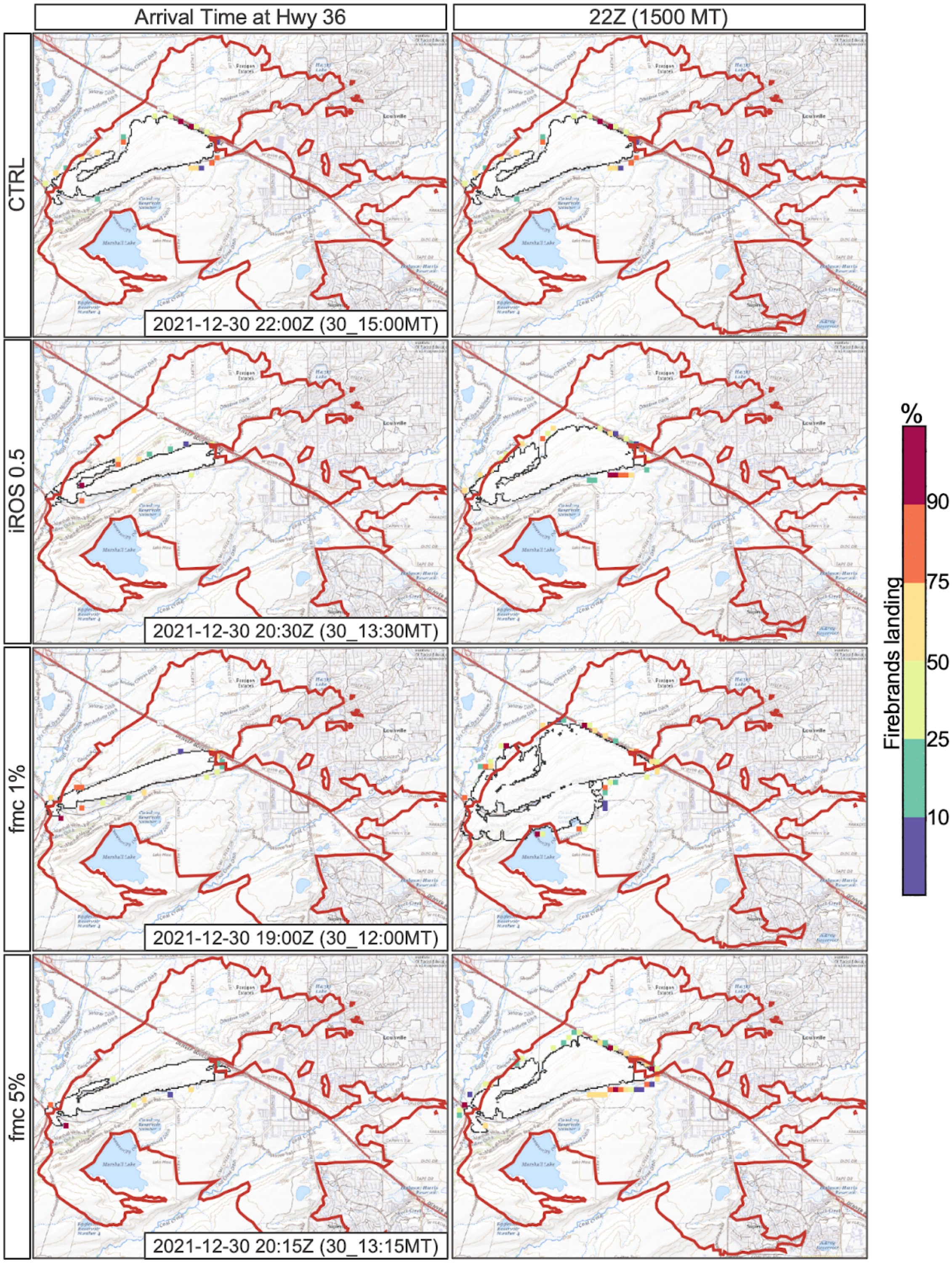

Figure 2. Model experiments showing sensitivities affecting the fire front arrival time at Hwy 36 (left), and the variability in fire spread and firebrands at 22Z (right). From top to bottom: CTRL, rate of spread at initialization (iROS 0.5), fuel moisture content of 1% (fmc 1%) and 5% (fmc 5%).

Supporting Information

Materials and Methods

The numerical simulations (1) were produced using WRF-ARW (2) v4.3.3 (develop branch, pre-release v4.4), configured with two nested domains, with 1000 and 111m of horizontal grid spacing, fixed 3-s time step, 45 vertical levels, fire grid refinement of 4, and boundary conditions from the High-Resolution Rapid Refresh (HRRR) model (3).

The model physics suite included the WRF Single-Moment 6-class scheme as the microphysics, RRTMG and Dudhia scheme for long and shortwave radiation, Yonsei University scheme for Planetary Boundary Layer, revised MM5 surface layer scheme, and Noah Land Surface Model (2).

The simulations were configured with Lambert projection centered at 39.967139, -105.364591 reference coordinates, outer domain size of x=164, y=160, and inner domain size of x=361, y=343 with ij start at 76 and 60.

WRF-Fire (4) was used for the fire behavior component. The Anderson 13-fuels layer used by WRF-Fire originates from the LANDFIRE database (5). The main fire was ignited from a 55-m line at an approximate location, near the locations under investigation by local authorities (39.956029, -105.230189). Ignition radius was set to 100-m, and start and end times to 300s and 600s, respectively.

The model parameters modified for multiple experiments included: number of ignitions, fire rate of spread at ignition time (fire_ignition_ros), and fuel moisture content (fuelmc_g). The experiments configurations followed those from CTRL with the following differentiation:

- CTRL: fire_ignition_ros = 0.05, fuelmc_g = 0.08.
- 4-spots: four additional point ignitions at the coordinates and times: (39.953964, -105.227496, 2400s); (39.958407, -105.207693, 6000s); (39.965521, -105.183354, 8700s); (39.969594, -105.193540, 11400s)
- iROS 0.05: fire_ignition_ros = 0.5
- fmc 1%: fuelmc_g = 0.01
- fmc 5%: fuelmc_g = 0.05

SI References

1. Computational and Information Systems Laboratory, Cheyenne: SGI ICE XA Cluster (2017) https:/doi.org/10.5065/D6RX99HX.
2. W. C. Skamarock, *et al.*, “A description of the advanced research WRF model version 4” (UCAR/NCAR, 2019) https:/doi.org/10.5065/1DFH-6P97.
3. B. K. Blaylock, J. D. Horel, S. T. Liston, Cloud archiving and data mining of High-Resolution Rapid Refresh forecast model output. *Comput. Geosci.* **109**, 43–50 (2017).
4. J. L. Coen, *et al.*, WRF-Fire: Coupled Weather–Wildland Fire Modeling with the Weather Research and Forecasting Model. *J. Appl. Meteorol. Climatol.* **52**, 16–38 (2013).
5. LANDFIRE, 13 Anderson Fire Behavior Fuel Models (LF 1.4.0) U.S. Department of Interior, Geological Survey, and U.S. Department of Agriculture. Dataset URL https://landfire.gov/fbfm13.php.